Picoseconds-Accurate Fiber-Optic Time Transfer With Relative Stabilization of Lasers Wavelengths

Łukasz Śliwczyński, *Member, IEEE*, Przemyslaw Krehlik, Łukasz Buczek, and Harald Schnatz

***Abstract*—In this paper we focus on analyzing the accuracy of time transfer in bidirectional fiber optic links. It has been pointed out that one of the main uncertainty contributions in such links is related to insufficient stabilization of the lasers' wavelengths and to the asymmetry of propagation caused by the fiber's chromatic dispersion. To reduce these contributions, we propose a scheme where the difference (offset) of the wavelengths of forward and backward lasers is stabilized and where optical interleavers are used as diplexers. This allows implementing a λ-swapping technique to assess dispersion-related link asymmetry during the link calibration. For the investigation of these approaches and the measurement of the associated stability we utilize a frequency-synchronized offset laser module (FSOLM) to realize an offset of 25 GHz. In this paper, we show that with the proposed λ-swapping technique the uncertainty associated with the propagation asymmetry due to fiber chromatic dispersion can be reduced to values below 2.5 ps for links up to 1000 km long, making it insignificant compared to other uncertainty contributions. A laboratory proof-of-concept experiment, in which distances up to 540 km were tested, showed good agreement between the measured and the anticipated propagation delay of investigated links.**

***Index Terms*—Calibration uncertainty, fiber optic, interleaver filter, laser wavelength stabilization, time transfer.**

I. Introduction

In RECENT years fiber optic time and frequency transfer techniques have become widespread across Europe and beyond, both in scientific and commercial applications. This is because traditional transfer schemes based on satellites are no longer sufficient to meet the requirements of users in terms of accuracy, stability, security, reliability and accessibility.

Currently the uncertainty of time transfer links based on global navigation satellite systems (GNSS) is typically around 2 ns [1] and a state-of-the-art method of calibrating receivers reached an uncertainty of 1 ns [2]. Two way satellite time and frequency transfer (TWSTFT) links, using geo-stationary satellites, realize an uncertainty below 1 ns [3]; they, however, require sophisticated equipment and trained staff.

Manuscript received March 22, 2020; revised May 8, 2020; accepted May 27, 2020. Date of publication June 1, 2020; date of current version September 15, 2020. This work was supported by the Polish National Science Center under Grant 2017/26/M/ST7/00128. *(Corresponding author: Łukasz Śliwczyński.)*

Łukasz Śliwczyński, Przemyslaw Krehlik, and Łukasz Buczek are with the AGH University of Science and Technology, Faculty of Computer Science, Electronics and Telecommunications, al. A. Mickiewicza 30, 30-059 Krakow, Poland (e-mail: sliwczyn@agh.edu.pl; krehlik@agh.edu.pl; lbuczek@agh.edu.pl).

Harald Schnatz is with the Physikalisch-Technische Bundesanstalt (PTB), Quantum Optics and the Unit of Length, Bundesallee 100, 38116 Braunschweig, Germany (e-mail: harald.schnatz@ptb.de).

Color versions of one or more of the figures in this article are available online at https://ieeexplore.ieee.org.

Digital Object Identifier 10.1109/JLT.2020.2999158

Fiber optic time transfer links, apart from being much more accurate, offer an alternative, which is often easier to implement, especially for links with stabilized propagation delay, and also easier to use and maintain. In addition, they do not require access to the satellite signals, which are not always detectable, e.g. in underground facilities or so-called urban canyons. Depending on the link length and the technology used, uncertainties in the range of 10 ps to below 1 ns [4]–[9] can be achieved.

The advantages of using optical fibers to perform time and frequency metrology are based on the inherent symmetry of the transmission medium, which allows almost perfect compensation of time delay or phase fluctuations when operated bidirectionally over the same optical fiber. This feature is e.g. absolute essential for optical clock comparisons and relativistic geodesy [10].

The possible range of applications of the fiber optic time transfer, apart from those related directly to the time scales generation and time metrology [4], [5], [11], [12], include telecommunications [13], [14], smart grid synchronization [15], astronomy [16], [17], nuclear physics [18] and even the financial sector [19], [20].

Each time transfer link is composed of two terminals that exchange an optical carrier modulated with one pulse per second (PPS) signals (in practice they are often associated with a radio frequency carrier). The link can be organized either in a two-way configuration (in analogy to TWSTFT) [4], or as a feedback system, [7], [8], which can stabilize the delay or the phase of the signal delivered to the remote end of such a link. Hybrid systems, intended to transfer RF, PPS and optical carrier [22]–[24], have also been investigated.

One of the specific aspects of time transfer, is the necessity of link calibration to determine the relation between the time scales at both ends of the link. This requires measurement of various delays associated with either the terminals or the optical fiber used to connect them [4]–[9]. This procedure is especially convenient in fiber optic links with stabilized propagation delay, where it can be performed from one side of the link only [5], [7], [13].

In the quest to achieve more accurate link calibrations, various aspects need to be taken into account. Typically, the uncertainty of link calibration increases with the length of the link; this is mainly because the fiber's chromatic dispersion causes residual asymmetry in the counter-propagating directions. This associated uncertainty contribution is usually substantial and can dominate the entire calibration [5], [13].

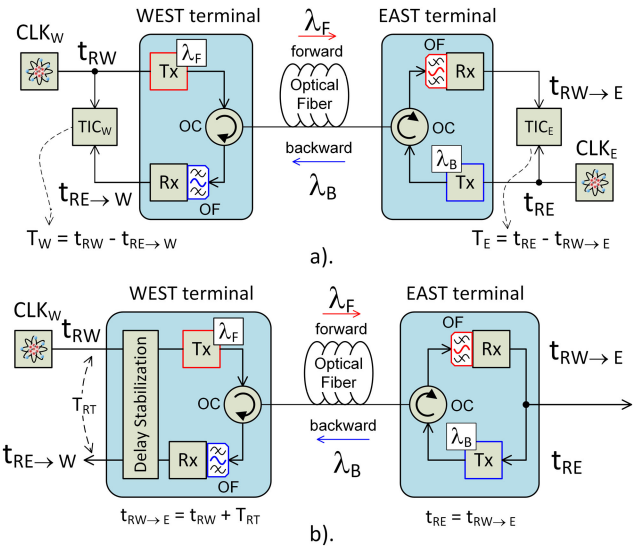

Fig. 1. General block diagram of fiber optic time transfer links: two-way (a) and stabilized propagation delay (b) architectures. Tx stands for the laser transmitter, Rx for optical receiver, OC for an optical circulator and OF is an optical band-pass filter.

There are approaches for reducing the aforementioned uncertainty contribution by using the same wavelengths to transmit signals in the forward and backward directions. This, however, is ineffective in links longer than a few tens of kilometers [25] unless special coding techniques [26] or amplification schemes requiring calibration of each amplifier [27] are implemented. This is due to problems with stray reflections and Rayleigh backscattering [28], which, for equal wavelengths, cannot be distinguished from the useful signals and generate a substantial amount of noise. In addition, the lasers operated in two physically separated locations can have only nominally equal wavelengths, so that the accuracy of their actual values is still associated with higher uncertainty values if a fiber link is operated in a wavelength region of non-zero chromatic dispersion, which is usually the case.

In this paper measures are proposed, analyzed and evaluated that make the calibration uncertainty due to the propagation delay asymmetry, related to fiber's chromatic dispersion, practically negligible and almost length-independent.

II. General Fiber-Optic Time Transfer Ideas and Their Accuracy

Let us first consider a generic fiber optic time transfer link, organized in a two-way configuration, shown schematically in Fig. 1(a). In this link the reference timing signals produced by two independent clocks, marked as $\mathrm{CLK_W}$ and $\mathrm{CLK_E}$, respectively, are exchanged between the west and east sites via corresponding west and east terminals, which are responsible for converting the signals from the optical to the electrical domain and vice versa. To assure that any fluctuations of the propagation delay of the transmission medium affect the transmitted signals equally in both directions, a single, bidirectionally operated fiber is used. When the length of the link exceeds some tens of kilometers, it is necessary to employ different wavelengths in the forward and backward directions, marked here as λ_F and λ_B, to circumvent the influence of the Rayleigh backscattering on the stability of transmitted signals.

The signals provided by the reference clocks (t_{RW} and t_{RE}, for the west and east ones, respectively), usually in form of one pulse per second (PPS), after transmitting to the other side of the link, can be expressed as:

$$t_{RW\to E} = t_{RW} - \tau_{IF} - \tau_F(\lambda_F), \tag{1}$$

$$t_{RE\to W} = t_{RE} - \tau_{IB} - \tau_B(\lambda_B), \tag{2}$$

where $\tau_F(\lambda_F)$ and $\tau_B(\lambda_B)$ are the forward and backward propagation delays of the fiber, with their wavelength dependence marked explicitly. Terms marked as τ_{IF} and τ_{IB} are used to account for all the instrumental delays (due to cables and electronics inside the terminals) of the forward and backward paths, respectively. Measuring the signals at both sides of the link using time interval counters (TIC) and then swapping the results allows a comparison of the two involved timescales:

$$t_{RW} - t_{RE} = \frac{T_W - T_E}{2} + \frac{\tau_C}{2} + \frac{\Delta\tau_{F\leftrightarrow B}}{2}, \tag{3}$$

where $T_W = t_{RW} - t_{RE\to W}$ and $T_E = t_{RE} - t_{RW\to E}$ are the readings of the TICs, $\tau_C = \tau_{IF} - \tau_{IB}$ is the calibration constant related to the asymmetry of propagation between the forward and backward directions inside the east and west terminals, and $\Delta\tau_{F\leftrightarrow B} = \tau_F(\lambda_F) - \tau_B(\lambda_B)$ is the asymmetry of propagation of the optical fiber due to its chromatic dispersion and other effects (see below).

The link with a stabilized propagation delay, shown schematically in Fig. 1(b), provides an "exact" copy of the timing signal from the west terminal to the east terminal, with stable and known propagation delay (after calibration). The signal at the east terminal can be obtained by putting $t_{RE} = t_{RW\to E}$ and observing that the feedback loop keeps the round-trip (i.e. from the west terminal to the east one and back) propagation delay T_{RT} constant. It is equal to:

$$t_{RW\to E} = \frac{T_{RT}}{2} + \frac{\tau_C}{2} + \frac{\Delta\tau_{F\leftrightarrow B}}{2} + t_{RW}. \tag{4}$$

Equations (3) and (4) show that the accuracy of time transfer in both approaches is influenced by similar factors. These are related to the accuracy of measuring time intervals T_W, T_E and T_{RT}, determining the asymmetry of terminals τ_C, and determining the propagation delay asymmetry $\Delta\tau_{F\leftrightarrow B}$. The limits on the accuracy due to the first two factors depend mostly on our capabilities of measuring the time intervals. Using a high-speed oscilloscope (like e.g. Keysight DSOS404 [29] or equivalent) or modern high-precision counters [30], [31] the uncertainty can be reduced to a few picoseconds only. In case of the delay-stabilized link the instrumental factor includes also the asymmetry of the matched delay lines, which, however, for custom-designed application specific integrated circuits (ASIC) can be at the level of 6–7 ps [7], [13]. This suggests that the contribution of the first two terms in (3) and (4) can be kept at less than 5 ps (with the sensitivity coefficient of $1/2$ included).

The asymmetry associated with the counter-propagating wavelengths is included in (3) and (4) as a few terms that affect

the accuracy of link calibration. The uncertainty contribution from the fiber birefringence can usually be neglected in current day fibers [5], however the contribution from the Sagnac effect and fiber's chromatic dispersion have to be taken into account. In this paper we will focus on this last factor as it is directly related to the fiber's properties and its uncertainty contribution can be optimized by proper design of the time transfer hardware. Accurate calculation of the Sagnac correction requires knowledge about the fiber's path and can be accounted for using appropriate models [6].

The propagation asymmetry caused by the chromatic dispersion can be expressed as:

$$\Delta\tau_{F\leftrightarrow B} = D_T \Delta\lambda_{F\leftrightarrow B}, \tag{5}$$

where $D_T = L \cdot D$ denotes the total chromatic dispersion of the entire L of the link, D is the chromatic dispersion coefficient and $\Delta\lambda_{F\leftrightarrow B} = \lambda_F - \lambda_B$. The accuracy of determining $\Delta\tau_{F\leftrightarrow B}$ depends critically on two aspects: the methods applied to stabilize the lasers' wavelengths and those to evaluate the chromatic dispersion.

The lasers used for time transfer applications are usually telecom-grade, distributed feedback (DFB) lasers, either stand alone or mounted within small form factor pluggable (SFP) modules. As phase coherence is not essential here, the wavelength of the laser is kept constant by either just laser temperature stabilization or by referencing the laser wavelength to a Fabry-Perot (F-P) etalon (i.e. a wavelength locker). Our extensive experience with these techniques shows that, after careful adjustment, accuracy at the level of ± 1 pm to ± 2 pm can be achieved. However, residual thermal sensitivity and component aging cannot be fully removed [32].

The total chromatic dispersion of the link can be obtained from either typical values or measured values of the chromatic dispersion coefficient, D, and the fiber length measured e.g. with an optical reflectometer (OTDR). To improve the accuracy, however, a preferred approach is to use a method with a calibrated laser shift. In its basic implementation the laser wavelength in one of the terminals (e.g. the west one) is detuned from its working value by a calibrated, known shift of $\Delta\lambda_M$ [5]. Using this approach (5) can be transformed to:

$$\Delta\tau_{F\leftrightarrow B} = \Delta\tau_M \frac{\Delta\lambda_{F\leftrightarrow B}}{\Delta\lambda_M}, \tag{6}$$

where $\Delta\tau_M$ is the change of the delay observed due to the change of the laser wavelength. An estimation of the accuracy of $\Delta\tau_{F\leftrightarrow B}$, based on (6) shows that it could dominate the uncertainty of entire transfer link. The lower limit is given by the multiplication of the uncertainty $u(\Delta\tau_M)$ by the ratio $\Delta\lambda_{F\leftrightarrow B}/\Delta\lambda_M$, which in practice can be between 2 and 3. This value results from the bandwidth limitation of the optical filter that needs to be placed prior the optical receiver to filter out the Rayleigh backscattering of the counter propagating signal (see Fig. 1). Then, the uncertainty $u(\Delta\tau_{F\leftrightarrow B})$ increases with the length of the fiber due to increase of $\Delta\tau_M$, reaching a level of 100 ps for distances at the order of 1000 km.

Thus, a more elaborate method of link calibration with the calibrated laser shift has been proposed [13]. It requires a two-step procedure with a long test fiber (ranging from 100 km to 300 km, depending on the required length of a time transfer link), which makes the calibration process more complex. However, the advantages are that the requirement of knowing exact values of $\Delta\lambda_M$ and $\Delta\lambda_{F\leftrightarrow B}$ are relaxed and the uncertainty is lower than in the basic version described in [5].

The analysis above shows that the factors limiting the calibration uncertainty of the fiber optic time transfer link are: 1). the quality of the lasers' wavelength stabilization and 2). the assessment of the asymmetry due to fiber chromatic dispersion.

The main idea, which is proposed and evaluated in this paper, is that for time transfer only a relative stability matters, that is the stability of the difference of the wavelengths (see (5)). It will thus be advantageous to lock the optical frequency of the laser in one of the terminals to the frequency of the other one (e.g. the east one to the west one) with a suitable offset between them. A similar approach is employed e.g. in regenerative laser stations (RLS) [33], developed for signal regeneration and distribution for long-haul optical carrier transfer systems to increase the link distance. In the case of the time transfer considered here, it is enough to have the lasers locked only with respect to frequency, as no optical coherence is needed. In addition, the bandwidth occupied by modulated optical signals is on the order of a few GHz, so it is mandatory that the offset conforms to the grid specified by International Telecommunication Union (ITU) for dense wavelength division multiplexing (DWDM) [34]. This way it is possible to use commercially available optical filters to separate the forward and backward signals.

III. Relative Wavelength Stabilization With a 25 GHz Offset

The availability of high-speed photodiodes with multi-GHz bandwidths and millimeter-wave integrated circuits (mixers, amplifiers, frequency dividers and microwave synthesizers) allows design of a compact laser subsystem with an offset in the range of several to several dozen of GHz relatively easily. In Fig. 2 such a frequency-synchronized offset laser module (FSOLM) for a 25 GHz offset is presented.

The laser used in our setup is a so-called integrable tunable laser assembly (ITLA) module, mainly because of its ease of tuning and versatility in selecting its frequency anywhere between 191.5 THz to 196.25 THz. This laser is compliant with a multisource agreement standard (MSA) and can be digitally tuned with the granularity of 1 MHz by programming its internal registers via a serial digital interface [35]. It also offers the possibility to define its own frequency grid and switching between the channels on the fly, which will be further exploited for determining the asymmetry of the fiber link due to fiber chromatic dispersion. The presented solution, however, will work equally well with any kind of single-mode laser (e.g. telecom grade DFB types), which can be tuned, e.g. by changing its temperature or current.

In the proposed scheme the beat note between the reference laser (ν_{Ref}) and the tunable one (ν_{TL}), equal to $f_{beat} =$

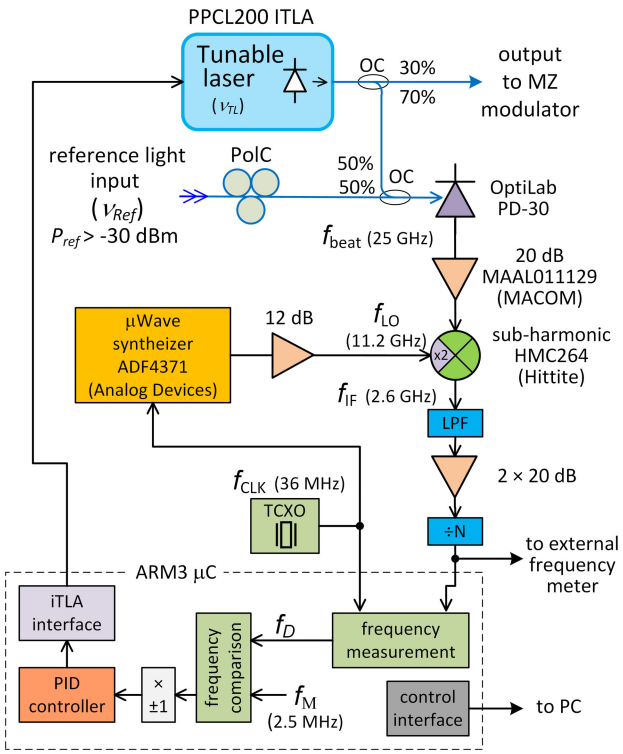

Fig. 2. Simplified block diagram of frequency-synchronized laser module with a 25 GHz offset to the reference laser. OC stands for optical coupler, MZ for Mach-Zehnder and PolC for polarization controller. Any mention of commercial products is for information only; it does not imply recommendation or endorsement by the authors.

$c \cdot \Delta\lambda_{F\leftrightarrow B}/\lambda_0^2$, where c denotes the speed of light and $\lambda_0 = (\lambda_F + \lambda_B)/2$, is detected in a high-speed photodiode (PD-30 from OptiLab) and is directed to a sub-harmonic (second order) mixer via a low-noise amplifier. The local port of the mixer is supplied from a microwave synthesizer with the output frequency equal to f_{LO}. The role of the mixer is to down-convert the high-frequency beat note to a frequency range, which, after further division by N using a chain of high-speed dividers, can be processed by a microcontroller (μC). In our case, we chose $f_{IF} = 2.6$ GHz, although this value is quite arbitrary. A low-pass filter (LPF) at the mixer output is used to reduce the crosstalk with the LO port, which was a source of a non-linear behavior of subsequent amplifiers.

The main task of the μC is to take the burden of frequency measurement (using its internal timers) and forming the control signal to ITLA using a proportional/integral/derivative (PID) algorithm. The μC is also responsible for communication with ITLA and the synthesizer, which needs initialization.

The entire system forms a frequency locked loop (FLL), where the divided beat frequency, f_D, is kept equal to f_M. This way the offset frequency between the lasers, f_{beat}, is stabilized and can be determined by the formula:

$$f_{beat} = \pm(N \cdot f_M + 2 \cdot f_{LO}), \tag{7}$$

which for the chosen values of f_{LO} of 11.2 GHz, f_M of 2.5 MHz and $N = 1040$ gives the desired offset value of 25 GHz. (Larger offsets are also possible but require higher-speed frontends that make system design more challenging.) The sign of the offset depends on the sign of the feedback loop, which can be changed in software via PC. This allows setting ITLA either above or below ν_{Ref}, which will be further exploited for determining $\Delta\tau_{F\leftrightarrow B}$.

Two components of the uncertainty of the beat frequency, $u(f_{beat})$, which corresponds to $u(\Delta\lambda_{F\leftrightarrow B})$, can be distinguished in the proposed scheme. The first one (type B) is related to the accuracy of the frequency of the clock oscillator driving the microwave synthesizer and timers inside the μC performing the frequency measurement. The second one (type A) is caused mainly by internal instability of ITLA and its tuning limitations.

Denoting the multiplication factor of the synthesizer as K, the type B uncertainty can be estimated as:

$$u_B(f_{beat}) = (2 \cdot K \cdot f_{CLK} + N \cdot f_M)\frac{\Delta f}{f}, \tag{8}$$

where $\Delta f/f$ is the relative uncertainty of f_{CLK}. Assuming $\Delta f/f = \pm 2.5$ ppm as characteristic for temperature compensated crystal oscillators (TCXO), allows an estimate of $u_B(f_{beat}) \approx 65$ kHz ($\sim 5{\cdot}10^{-5}$ pm).

The type A uncertainty of the described FSOLM was evaluated in the laboratory by measuring the stability of f_{beat}. As this frequency is too high to conveniently perform a direct measurement, we assessed the signal at the output of the N-divider using a K+K FXE-80 phase and frequency meter (see Fig. 2). The setup we used in this measurement comprised a RIO Planex laser module as a source of remote optical frequency set for $\nu_{Ref} = 193.5125$ THz, modulated using an external Mach-Zehnder (MZ) modulator, driven by the signal conveying the time and RF frequency. The signal from the modulator, after attenuating it to -20 dBm, was applied to the input of the considered FSOLM.

The results registered over five days, after multiplying by N to compensate for the effect of the divider, are shown in Fig. 3(a). The root-mean-square (RMS) value of the fluctuations, which can be used as an estimate of $u_A(f_{beat})$, is around 7.6 MHz (that corresponds to 0.06 pm) and results mainly from the above mentioned granularity of ITLA tuning of 1 MHz and its relatively slow response of $\sim$1s.

The same measurement, repeated with the laser stabilization loop disabled, showed slow and large wander of ITLA frequency with its RMS value around 190 MHz (Fig. 3(b)). The 25-fold improvement of stability, together with a symmetric, Gaussian-like distribution of fluctuations, showed no signs of jumps or trends with the stabilization loop activated (see histograms in Fig. 3(a)), demonstrating the proper implementation and operation of the FSOLM. The measurements were repeated for both positive and negative offsets with respect to ν_{Ref}, and showed similar performance of the investigated circuit in each case.

Based on (6) one can estimate the joint contribution of both type A and type B uncertainties of f_{beat} to the uncertainty of determining $\Delta\tau_{F\leftrightarrow B}$ as being on the order of 1.2 ps, even for a 1000 km long fiber link. This result of 1.2 ps demonstrates that a calibration of time transfer link is not limited by laser-related issues, like their relative inaccuracy and/or instability.

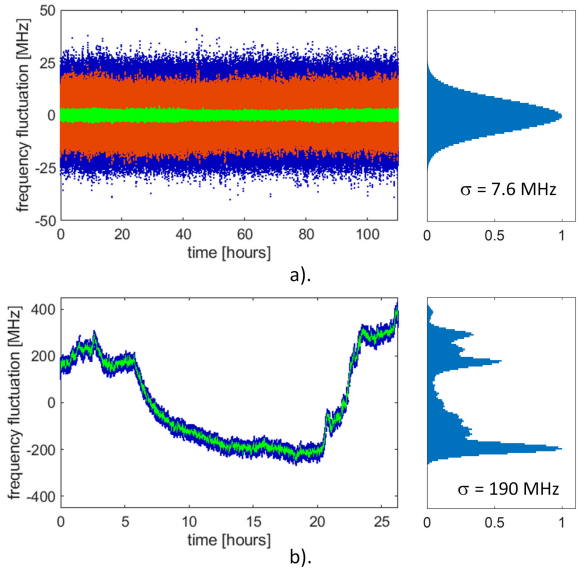

Fig. 3. Fluctuations of the frequency ν_{TL} of the FSOLM measured against ν_{Ref}: with stabilization loop activated (a), and deactivated (b). The red and green overlays show a moving average calculated over 1 s and 10 s, respectively. The right part of the figure shows the histograms.

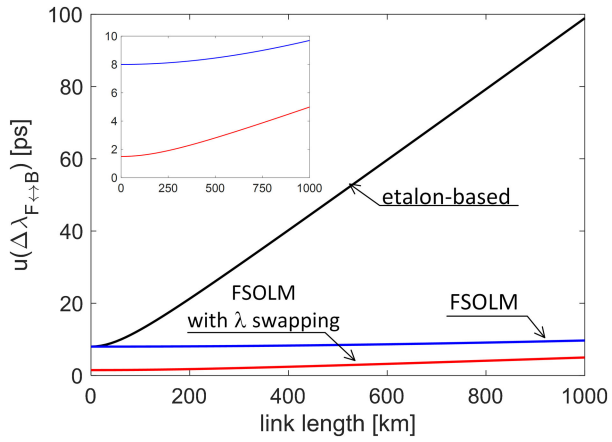

Fig. 4. Comparison of the uncertainty related to the propagation asymmetry due to chromatic dispersion. The inset shows zoomed plots for the FSOLM and FSOLM with the λ-swapping cases.

IV. Uncertainty Related to Link Asymmetry

The uncertainty associated with link asymmetry caused by chromatic dispersion has to take into account the thermal dependence of chromatic dispersion. This can easily be done by modifying the basic equation (6):

$$\Delta\tau_{F\leftrightarrow B} = \Delta\tau_M \frac{\Delta\lambda_{F\leftrightarrow B}}{\Delta\lambda_M}\left(1+\frac{1}{D}\frac{dD}{dT}\Delta T\right), \qquad (9)$$

where ΔT is the temperature change and dD/dT is the chromatic dispersion thermal sensitivity.

The uncertainties calculated with (9) for the wavelength stabilization schemes, using either an optical etalon or FSOLM are shown in Fig. 4 with black and blue lines, respectively. (The case named λ-swapping, also shown in the figure, is discussed in the next section.) The calculation results plotted for Fig. 4 assume a standard singlemode fiber (SMF) with $D = 17$ ps·nm^{-1}·km^{-1} and $dD/dT = 4$ fs nm^{-1}·km^{-1} K^{-1}. The ratio $\Delta\lambda_{F\leftrightarrow B}/\Delta\lambda_M = 2.67$ is used and ΔT of 20 °C is assumed. The uncertainties $u(\Delta\lambda_{F\leftrightarrow B})$ and $u(\Delta\lambda_M)$ were assumed to be equal, with values of 2 pm and 0.06 pm for etalon-based and FSOLM schemes, respectively. An uncertainty of the time interval measurement of $u(\Delta\tau_M) = 3$ ps, results in the uncertainty $u(\Delta\tau_{F\leftrightarrow B})$ of less than 10 ps for the FSOLM case, which, furthermore, appears to be almost independent of the link length. This is a substantial improvement comparing to the etalon-based scheme.

V. Improved In-situ Assessment of Link Asymmetry

The uncertainty values for FSOLM presented above are low; however, there is still room for improvement. The idea that is proposed in the following is to use a pair of optical interleavers as diplexers (see Fig. 5(a)) instead of using optical circulators and filters in the time transfer schemes shown in Fig. 1. Such an interleaver has a comb characteristic and is a standard tool for multiplexing and de-multiplexing lightwave traffic in telecommunications applications with grids supporting frequencies less than 50 GHz, for which single channel DWDM filters are difficult to manufacture. In our application, the advantage of interleavers is that their use allows substantial increase of $\Delta\lambda_M$ compared to the typical DWDM filter. This is because, in this approach, tuning of the laser during the measurement of the asymmetry of propagation delay caused by the chromatic dispersion is not limited by the bandwidth of the filter, but can be done using consecutive interleaver channels (each one corresponding to the single comb of the interleaver characteristics) and swapping the laser wavelength between them. In this way the sensitivity coefficient associated with $u(\Delta\tau_M)$, which equals to $\Delta\lambda_{F\leftrightarrow B}/\Delta\lambda_M$ (see (9)), can be reduced from its typical value around 2.5 to as low as 0.5.

There are two possible approaches to implementing the above-mentioned idea of λ-swapping. In the first of them, shown in Fig. 5(b), the wavelength of one of the lasers, e.g. λ_B, is symmetric with respect to the other one (i.e. λ_F), giving the net change of the wavelength $\Delta\lambda_M = 2\cdot\Delta\lambda_{F\leftrightarrow B}$. The same net change can also be obtained using the second approach, shown in Fig. 5(c), where during the measurement of $\Delta\tau_M$ the lasers wavelengths are exchanged. The first approach consumes more optical bandwidth and, in addition, requires taking into account the non-zero dispersion slope S of the optical fiber, because the estimation of dispersion is performed at a different wavelength than $\lambda_D = (\lambda_F + \lambda_B)/2$. This, however, can be easily included by multiplying (9) by another correction term, equal to $(1 - S/D\cdot\Delta\lambda_{F\leftrightarrow B})$. Typical values of S in the vicinity of 1550 nm are equal to 0.058 ps·nm^{-2}·km^{-1}, 0.045 ps·nm^{-2}·km^{-1} and 0.085 ps·nm^{-2}·km^{-1} [36] for SMF, non-zero dispersion shifted (NZDSF) and large effective area (LEAF) fibers, respectively. The value of the correction factor is close to one, but needs to be taken into account for calibration at the picosecond level. This is especially true for NZDSF or LEAF fibers where the error resulting from omitting this correction is ∼2 ps and ∼4 ps for a 500 km long link, respectively (assuming $\Delta\lambda_{F\leftrightarrow B} = 0.2$ nm). For the SMF fiber an error of ∼1 ps is expected. As the approach

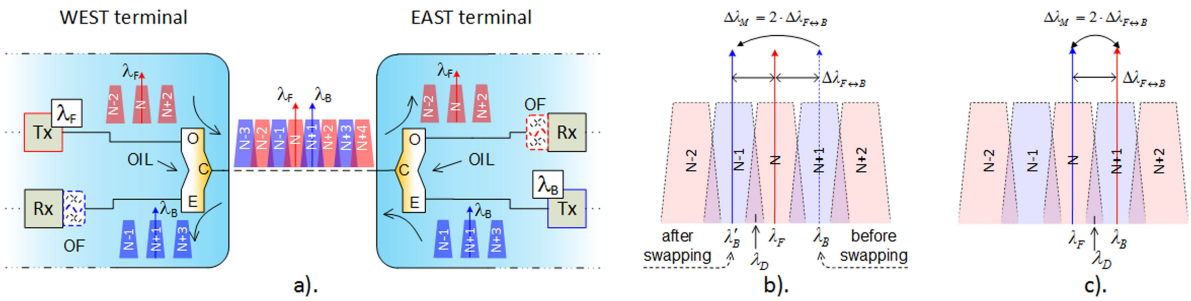

Fig. 5. Idea of fiber optic transfer scheme with optical interleavers used as diplexers (a), possible schemes of shifting lasers frequencies during assessing the symmetry of the fiber link due to the chromatic dispersion (b) and (c). In the figure C, O and E are used to denote common, odd and even optical ports of the interleaver (OIL).

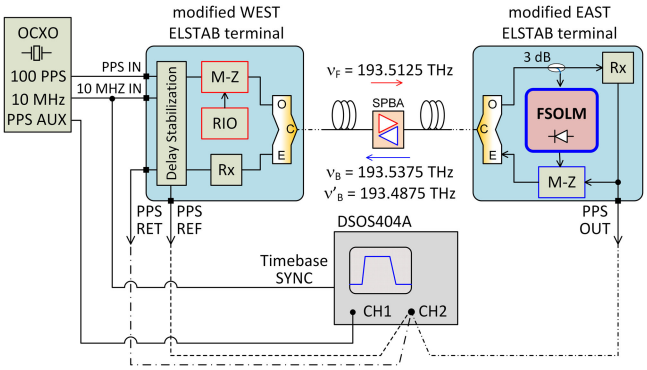

Fig. 6. Experimental setup used to verify the calibration accuracy of time transfer.

of Fig. 5(b) is easier to implement (only one of the lasers needs to be tuned) we decided to use it in the experiments described in the next section.

The uncertainty of $\Delta\tau_{F\leftrightarrow B}$ using λ-swapping is drawn with red color in Fig. 4, taking $\Delta\lambda_M = 2\cdot\Delta\lambda_{F\leftrightarrow B}$. In comparison to the case using just FSOLM alone, a reduction by a factor of two to five, depending of the link length, is noticeable. The resulting uncertainty $u(\Delta\tau_{F\leftrightarrow B})$ is thus below 5 ps even for a 1000 km long link. This way we reached a state where the calibration of time transfer link is limited by neither the lasers' stability, nor their wavelength accuracy. The residual length dependence of $u(\Delta\tau_{F\leftrightarrow B})$ is caused by a non-zero thermal coefficient of chromatic dispersion – if required this effect can be reduced by decreasing the spacing between the forward and backward directions from 25 GHz to e.g. 12.5 GHz.

VI. Experimental Verification of Calibration

To confirm the predictions presented in the previous sections we performed a proof of concept experiment, where the calibration of a stabilized time transfer link was compared with the direct measurement of its propagation delay. For this experiment we employed a technology known as ELSTAB for electronically stabilizing the propagation delay of the fiber link [7], with both west and east terminals co-located in the same laboratory to make the comparison possible.

The experimental setup is shown in Fig. 6. It is composed of two modified ELSTAB terminals, where the optical circulators and filters have been replaced with interleavers (25/50GHz by Optoplex) and the optical transmitters use external M-Z modulators, together with required stabilization electronics. In the east (remote) ELSTAB terminal, the FSOLM with a $\pm$25 GHz offset, as described in Section III, was installed. This setup was tested over the distances ranging from 50 km up to about 540 km, composed of spooled and field-deployed underground fibers. Between the spans, a suitable number of single path bidirectional optical amplifiers (SPBA) [5], [7] were inserted to compensate for the losses. The optical power reaching the input of the east terminal was kept at the level of around -28 dBm.

The measurements were performed relative to the reference port (PPS_REF) of the west ELSTAB module, where the signal marking the exact time instant of the PPS pulse transmission is available. We used a high-speed digital oscilloscope with a sampling rate of 20 GHz and bandwidth above 4 GHz (Keysight DSOS404A) to measure time intervals. To remove uncertainty contributions associated with the oscilloscope time base, we synchronized the oscilloscope from the same generator, driven by a 10 MHz oven controlled crystal oscillator (OCXO), which served as the source of PPS and 10 MHz signals being the inputs to ELSTAB system. The oscilloscope was triggered from an auxiliary PPS output of the generator, which was synchronized with the main PPS output and delayed by a constant delay. To speed up the measurements we employed a 100 PPS reference instead of the usual 1 PPS reference.

The measurement done for each fiber span was composed of a few phases. First, the oscilloscope was calibrated by connecting its input (channel 2) to the PPS_REF port of the west ELSTAB terminal and the skew between channels 1 and 2 was adjusted to set the position of the PPS rising edge to zero. This way we compensated for the delays introduced by the cables and removed any internal skew of the oscilloscope. Next, we used the same cable to measure the round-trip (T_{RT}) and the propagation ($\tau^{measured}_{REF\rightarrow OUT}$) delays by connecting the PPS_RET and PPS_OUT ports to the oscilloscope, respectively. In the last step, we measured the asymmetry $\Delta\tau_{F\leftrightarrow B}$ due to fiber chromatic dispersion. This was done by deactivating the stabilization loop of the ELSTAB system and measuring the change of the round-trip signal in response to switching the FSOLM frequency from ν_B to ν'_B, as was described in Section IV. Due to the impact of temperature changes on the delay of fiber under the open-loop conditions required for the $\Delta\tau_{F\leftrightarrow B}$ measurements, we made a

TABLE I
RESULTS OF EXPERIMENTAL VERIFICATION OF TIME CALIBRATION

№	length [km] (a)	T_{RT} [ps] (b)	$\Delta\tau_{F\leftrightarrow B}$ [ps] (c)	$\tau^{measured}_{REF\rightarrow OUT}$ [ps] (d)	$\tau^{calculated}_{REF\rightarrow OUT}$ [ps] (e)	difference [ps] (f)	comments (g)
1	50	496730497±8	-161±4	248370374±8	248370373±8	-1±11	1 spool
2	100	992060498±8	-323±4	496035293±8	496035292±8	-1±11	2 spools, 1×SPBA
3	140	1209920497±8	-394±4	604965261±8	604965256±8	+5±11	2×70 km field deployed, 1×SPBA
4	150	1487350496±8	-485±4	743680210±8	743680210±8	0±11	3 spools, 2×SPBA
5	200	1982660498±8	-644±4	991335129±8	991335132±8	-3±11	4 spools, 3×SPBA
6	250	2478000498±8	-802±4	1239005052±8	1239005052±8	0±11	5 spools, 4×SPBA
7	300	2973250493±8	-960±4	1486629973±8	1486629971±8	+2±11	6 spools, 5×SPBA
8	350	3468570490±8	-1123±4	1734289886±8	1734289888±8	-2±11	7 spools, 6×SPBA
9	400	3963770496±8	-1283±4	1981889814±8	1981889811±8	+3±11	8 spools, 7×SPBA
10	420	4072870493±8	-1322±4	2036439786±8	2036439790±8	-4±11	7 spools + 70 km field deployed, 7×SPBA
11	470	4677240493±8	-1518±4	2338624689±8	2338620192±8	-3±11	8 spools + 70 km field deployed, 8×SPBA
12	540	5172590497±8	-1678±4	2586299610±8	2586299614±8	-4±11	8 spools + 2×70 km field deployed, 9×SPBA

series of 10 measurements to detect and further remove any resulting trend that otherwise would affect the measurement accuracy. The uncertainty contribution associated with this issue is below 1 ps after trend compensation and can be neglected in our case. The problem is minimal for underground fibers, but is significant when using spooled fibers in the laboratory.

To measure the position of the rising edge of PPS pulses, we sought for the crossing with a reference level, set in the middle of the pulse amplitude and then, with help of the histogram option of the oscilloscope, we found the mean value of the registered crossings. The results of the measurements are summarized in Table I.

The calibration formula, which was used to calculate the anticipated value of the link propagation delay shown in column (e), is based on (4) and reads:

$$\tau^{calculated}_{REF\rightarrow OUT} = \frac{T_{RT}}{2} + \frac{\tau_C}{2} + \frac{\Delta\tau_{F\leftrightarrow B}}{2}. \tag{10}$$

The value of the calibration constant τ_C was measured with both the west and east terminals connected with a short patchcord as equal to 10409 ps with $u(\tau_C) = 6.5$ ps. The uncertainties of measuring time delays using the oscilloscope were estimated based on the manufacturer's data as $u(\tau_{REF\rightarrow RET}) = u(\tau^{measured}_{REF\rightarrow OUT}) = 4$ ps. Based on Fig. 4 and taking $u(\Delta\tau_{F\leftrightarrow B}) = 3$ ps, one can get the combined uncertainty of the link calibration, $u(\tau^{calculated}_{REF\rightarrow OUT})$, as equal to about 4 ps. The expanded uncertainty shown in Table I in columns (b) to (f) use a typical expansion coefficient of 2, corresponding to a coverage interval of 95%.

The main result of this experiment is presented in column (f). This shows the difference between the measured and anticipated delays of examined links. This difference is below 5 ps in each case and it is well within the limits of the estimated expanded uncertainty. This proves that using FSOLM with the λ-swapping can offer high accuracy time transfer over the distances covering hundreds of kilometers.

VII. CONCLUSION

The factors that limit the accuracy of time transfer using fiber optic links can be divided into two categories, one related to the accuracy of time interval measurements and the other to the stability of lasers' wavelengths and the ability to assess the asymmetry of propagation due to fiber chromatic dispersion. In practice it appears that the latter one dominates in the case where the lasers' wavelengths are stabilized based on an etalon. The technique of stabilizing the difference of the wavelengths used for the forward and backward directions based on FSOLM, which is investigated here, proved to be a viable solution to overcome this limitation. The improvement compared to the link without the described technique, is about an order of magnitude.

Implementation of interleavers as diplexers in a bidirectional link allows applying the λ-swapping technique, which can further reduce the uncertainty of the calibration because it much larger frequency shift that can be applied to the laser during the asymmetry assessment. This allows an additional factor of between two to five (depending on link length) in improvement of the accuracy of determining $\Delta\tau_{F\leftrightarrow B}$. Any further improvement would require employing more accurate methods of time interval measurement because the calibration uncertainty is now limited primarily by the first two terms in (3) and (4).

The proposed methods, although tested here with ELSTAB, can be used in any fiber optic transfer link exploiting bidirectional transmission over the same fiber (using, e.g. a two-way approach). They are certainly more complex than a standard approach based on direct wavelength stabilization, but the implementation of both proposed ideas, as proposed here, practically eliminates the impact of $u(\Delta\tau_{F\leftrightarrow B})$ and the dominant uncertainty contributions come from the equipment used to conduct the time interval measurement. In addition, the proposed approach assures a long-term stability of the lasers' wavelength-difference, which cannot be fully guaranteed in any of standard approaches where wavelength stabilization is performed independently in each terminal.

It should be pointed out that for time transfer purposes only the stabilization of the relative frequency offsets between the lasers is required and no phase coherence is needed. This substantially reduces the requirements concerning the selection of suitable laser sources, simplifies the system design and reduces costs.

The proposed setup can be further improved in two independent aspects. One aspect is related to improving the short-term stability, which requires upgrading the laser in the FSOLM. This can be done either by using ITLA equipped with a piezo-electric transducer (e.g. PPCL300 from PurePhotonics) or a narrowband laser, like e.g. the RIO Planex. The other aspect concerns increasing the sensitivity of the FSOLM, which is now limited to about -30 dBm by internal noise of the electronics. For the application considered in this paper, the current sensitivity of the FSOLM is satisfactory, but it can be further improved by either reducing the bandwidth of the microwave processing chain, which is now about 3.5 GHz, or by implementing an image rejection mixer to reduce the contribution of noise originating in the resistor terminating the photodiode.

ACKNOWLEDGMENT

The authors would like to thank Jochen Kronjaeger from the National Physical Laboratory (UK) for bringing our attention to optical interleavers as possible filters for removing Rayleigh backscattering noise in narrowly-spaced bidirectional fiber links.

REFERENCES

[1] H. Esteban, J. Palacio, F. J. Galindo, T. Feldmann, A. Bauch, and D. Piester, "Improved GPS-based time link calibration involving ROA and PTB," *IEEE Trans. Ultrason. Ferroelect. Freq. Control*, vol. 57, no. 3, pp. 714–720, Mar. 2010.

[2] D. Valat and J. Delporte, "Absolute calibration of timing receiver chains at the nanosecond uncertainty level for GNSS time scales monitoring," *Metrologia*, vol. 57, 2020, Art. no. 025019.

[3] Z. Jiang *et al.*, "Improving two-way satellite time and frequency transfer with redundant links for UTC generation," *Metrologia*, vol. 56, 2019, Art. no. 025005.

[4] M. Rost *et al.*, "Time transfer through optical fibers over a distance of 73 km with an uncertainty below 100 ps," *Metrologia*, vol. 49, pp. 772–778, 2012.

[5] Ł. Sliwczynski *et al.*, "Dissemination of time and RF frequency via a stabilized fibre optic link over a distance of 420 km," *Metrologia*, vol. 50, pp. 133–145, 2013.

[6] J. Gersl, P. Delva, and P. Wolf, "Relativistic corrections for time and frequency transfer in optical fibers," *Metrologia*, vol. 52, pp. 552–564, 2015.

[7] P. Krehlik, L. Sliwczyski, L. Buczek, J. Kolodziej, and M. Lipinski, "ELSTAB- fiber optic time and frequency distribution technology - A general characterization and fundamental limits," *IEEE Trans. Ultrason. Ferroelect. Freq. Control*, vol. 63, no. 7, pp. 993–1004, Jul. 2016.

[8] M. Lipiński, T. Włostowski, J. Serrano, and P. Alvarez, "White rabbit: A PTP application for robust sub-nanosecond synchronization," in *Proc. 2011 IEEE Int. Symp. Preci. Cloc. Synchroniz. Meas., Contr. Commun.*, Munich, Germany, 2011, pp. 25–30.

[9] E. Dierikx *et al.*, "White rabbit precision time protocol on long-distance fiber links," *IEEE Trans. Ultrason. Ferroelectr. Freq. Control*, vol. 63, no. 7, pp. 945–952, Jul. 2016.

[10] T. Mehlstäubler, G. Grosche, Ch. Lisdat, P. Schmidt, and H. Denker, "Atomic clocks for Geodesy," *Rep. Prog. Phys.*, vol 81, 2018, Art. no. 064401.

[11] Z. Jiang, A. Czubla, J. Nawrocki, W. Lewandowski, and E. F. Arias, "Comparing a GPS time link calibration with an optical fibre self-calibration with 200 ps accuracy," *Metrologia*, vol. 52, pp. 384–391, 2015.

[12] J. Kodet *et al.*, "Two-way time transfer via optical fiber providing subpicosecond precision and high temperature stability," *Metrologia*, vol. 53, 2016, Art. no. 18.

[13] Ł. Śliwczyński *et al.*, "Calibrated optical time transfer of UTC(k) for supervision of telecom networks," *Metrologia*, vol. 56, 2019, Art. no. 015006

[14] Ł. Śliwczyński *et al.*, "Fiber-based UTC dissemination supporting 5G telecommunications networks," *IEEE Commun. Mag.*, vol. 58, no. 4, pp. 67–73, Apr. 2020.

[15] J. Gutierrez-Rivas, J. Lopez-Jimenez, E. Ros, and J. Diaz, "White rabbit HSR: A seamless subnanosecond redundant timing system with low-latency data capabilities for the smart grid," *IEEE Trans. on Ind. Inform.*, vol. 14, no. 8, pp 3486–3494, Aug. 2018.

[16] J. Lopez-Jimenez, F. Torres-Gonzales, J. Gutierrez-Rivas, M. Rodriguez-Gonzales, and J. Diaz, "A fully programmable White-Rabbit node for the SKA telescope PPS distribution system," *IEEE Trans Instrum. Meas.*, vol. 68, no. 2, pp. 632–641, Feb. 2019.

[17] S. Schediwy *et al.*, "The mid-frequency square kilometre array phase synchronisation system," *Publisher. Astronomical. Soc. Australia.*, vol. 36, 2019, Paper e007.

[18] C. de la Morena *et al.*, "Fully digital and White Rabbit-synchronized low-level RF system for LIPAc," *IEEE Trans. Nucl. Sci.*, vol, 65, no. 1, pp. 514–522, Jan. 2018.

[19] NPLTime, National Physical Laboratory, U.K. [Online]. Available: https://www.npl.co.uk/npltime

[20] J. López-Jiménez, J. Gutiérrez-Rivas, E. Marín-López, M. Rodríguez-Álvarez, and J. Díaz, "Time as a service based on White Rabbit for finance applications," *IEEE Commun. Mag.*, vol. 58, no. 4, pp. 60–66, Apr. 2020.

[21] C. Gao *et al.*, "Fiber-based multiple-access ultrastable frequency dissemination," *Opt. Lett.*, vol. 37, pp 4690–4692, 2012.

[22] S. M. F. Raupach and G. Grosche, "Chirped frequency transfer: A tool for synchronization and time transfer," *IEEE Trans. Ultrason., Ferroelect., Freq. Control*, vol. 61, no. 6, pp. 920–929, Jun. 2014.

[23] O. Lopez *et al.*, "Simultaneous remote transfer of accurate timing and optical frequency over a public fiber network," *Appl. Phys. B*, vol. 110, no. 1, pp. 3–6, 2013.

[24] P. Krehlik, H. Schnatz, and Ł. Śliwczyński, "A hybrid solution for simultaneous transfer of ultrastable optical frequency, RF frequency and UTC time-tags over optical fiber," *IEEE Trans. Ultrason. Ferroel. Freq. Contr.*, vol. 64, no. 12, pp. 1884–1890, Dec. 2017.

[25] Ł. Śliwczyński, P. Krehlik, and M. Lipiński, "Optical fibers in time and frequency transfer," *Meas. Sci. Technol.*, vol. 21, 2010, Art. no. 075302.

[26] G. Wu, L. Hu, H. Zhang, and J. Chen, "High-precision two-way optic-fiber time transfer using an improved time code," *Rev. Sci. Instrum.*, vol. 85, 2014, Art. no. 114701.

[27] H. Zhang, G. Wu, L. Hu, X. Li, and J. Chen, "High-precision time transfer over 2000-km fiber link," *IEEE Photon. J.*, vol. 7, no. 6, Dec. 2015, Art. no. 7600208.

[28] P. Wan and J. Conradi, "Impact of double Rayleigh backscatter noise on digital and analog fiber systems," *J. Lightw. Technol.*, vol. 14, no. 3, pp. 288–297, Mar. 1996.

[29] Infiniium S-series Oscilloscopes Data Sheet, Keysight, 2019. [Online]. Available: https://www.keysight.com

[30] R. Szplet, Z. Jachna, P. Kwiatkowski, and K. Różyc, "A 2.9 ps equivalent resolution interpolating time counter based on multiple independent coding lines," *Meas. Sci. Technol.*, vol. 24, 2013, Art. no. 035904.

[31] R. Szplet, R. Szymanowski, and D. Sondej, "Measurement uncertainty of precise interpolating time counters," *IEEE Trans. Instr. Meas.*, vol. 68, no. 11, pp. 4348–4356, Nov. 2019.

[32] Athermal Fabry-Perot Wavelength Locker, Optoplex Corporation. [Online]. Available: https://www.optoplex.com

[33] F. Guillou-Camargo *et al.*, "First industrial-grade coherent fiber link for optical freqency standard dissemination," *Appl. Opt.*, vol. 57, pp. 7203–7210, 2018.

[34] "Spectral grids for WDM applications: DWDM frequency grid," ITU-T Recommendation G.694.1, 2012. [Online]. Available: https://www.itu.int

[35] Integrable Tunable Laser Assembly Multi Source Agreement, Document OIF-ITLA_MSA-01.3, Optical Internetworking Forum, 2015. [Online]. Available: https://www.oiforum.com

[36] K. Aikawa *et al.*, "High performance dispersion and dispersion slope compensating fiber modules for non-zero dispersion shifted fibers," Fujikura Technical Review no. 32, pp. 5–10, 2003.